NASA TECHNICAL NOTE

NASA TN D-2076

NASA TN D-2076

EXPERIMENTAL INVESTIGATION OF A 4.54-INCH-MEAN-DIAMETER THREE-STAGE REVERSE-FLOW REENTRY TURBINE

by Donald E. Holeski and William T. Wintucky

Lewis Research Center

Cleveland, Ohio

NATIONAL AERONAUTICS AND SPACE ADMINISTRATION • WASHINGTON, D. C. • NOVEMBER 1963

TECHNICAL NOTE D-2076

EXPERIMENTAL INVESTIGATION OF A 4.54-INCH-MEAN-DIAMETER THREE-STAGE REVERSE-FLOW REENTRY TURBINE

By Donald E. Holeski and William T. Wintucky

Lewis Research Center
Cleveland, Ohio

NATIONAL AERONAUTICS AND SPACE ADMINISTRATION

EXPERIMENTAL INVESTIGATION OF A 4.54-INCH-MEAN-DIAMETER THREE-STAGE REVERSE-FLOW REENTRY TURBINE

By Donald E. Holeski and William T. Wintucky

SUMMARY

A three-stage 4.54-inch-mean-diameter reverse-flow reentry turbine was designed and evaluated experimentally in cold air. This turbine was designed for a blade- to jet-speed ratio of 0.244, a total- to static-pressure ratio of 14.5, and a rotative speed of 22,436 rpm.

At design speed and pressure ratio, the equivalent specific work output obtained was 38 Btu per pound at a static efficiency of 0.57, which compare to design values of 41.8 and 0.63, respectively. A single-stage test of the turbine showed that, because of overexpansion, the first stage produced slightly more than its design work. A study of the weight-flow variations through the turbine affected by leakage flows is also presented.

INTRODUCTION

As part of an NASA research program on turbines of high specific work and low weight flow, a three-stage reentry turbine was designed, fabricated, and evaluated experimentally in cold air. The turbine had a 4.54-inch mean diameter and was designed for requirements in the general area of small pump drives for rocket propellants. Multistaging was accomplished by passing air through a single rotor three times. This turbine is defined as a reverse-flow type because air movement through the second stage is in the opposite direction to air movement in the first and third stages. This type of a turbine may also be referred to as a cross-flow reentry turbine.

Descriptions and advantages of reentry turbines are given in previous NASA reports (refs. 1 to 4). The following are the primary advantages of reentry turbines. The later stages act to cool the single rotor and, thus, to maintain lower rotor-blade operating temperatures in the initial stages than in similar stages in full-admission turbines. Higher inlet temperatures therefore can be used for a given maximum rotor-blade operating temperature, which results in higher power output per pound of fuel expended. Reentry turbines permit longer rotor-blade heights than full-admission turbines for the same applications. The use of a single rotor gives a lighter and less complex rotating assembly.

This report presents information on the turbine design and the results of

evaluating the turbine experimentally with cold air as the driving fluid. The experimental investigation was conducted by (1) investigating the complete unit and (2) evaluating the first-stage performance alone to determine the percentage of the total work being produced by the first stage. A study of the weight-flow variation through the turbine was also made to gain knowledge of the internal flow leakage.

SYMBOLS

A	cross-sectional inlet area, sq ft
c	rotor-blade chord, in.
g	gravitational constant, 32.17 ft/sec^2
Δh	specific work output, Btu/lb
J	mechanical equivalent of heat, 778.16 ft-lb/Btu
l	rotor-blade height, in.
N	turbine speed, rpm
P	absolute pressure, lb/sq ft
R	gas constant, 53.35 ft-lb/^{o}R
T	absolute temperature, ^{o}R
U	blade velocity, ft/sec
V	absolute gas velocity, ft/sec
W	relative gas velocity, ft/sec
w	weight flow, lb/sec
α	absolute gas-flow angle measured from tangential direction, deg
β	relative gas-flow angle into and out of rotor measured from tangential direction, deg
γ	ratio of specific heats
δ	ratio of inlet total pressure to U.S. standard sea-level pressure, P'/P^*

ϵ function of γ used in relating weight flow to that using inlet conditions at U.S. standard sea-level atmosphere,

$$\frac{0.740}{\sqrt{\gamma}}\left(\frac{\gamma+1}{2}\right)^{\frac{\gamma}{\gamma-1}}$$

η_s static efficiency, ratio of blade power to ideal blade power based on total- to static-pressure ratio

θ_{cr} squared ratio of critical velocity at turbine inlet to critical velocity at U.S. standard sea-level temperature, V'_{cr}/V^*_{cr}

λ speed-work parameter, $\frac{U_m^2}{gJ\,\Delta h}$

ν blade- to jet-speed ratio, $\frac{U_m}{\sqrt{2gJ\,\Delta h_{id}}}$

ρ_{av} average stage density, lb/cu in.

Φ ratio of rotor-channel area to sum of rotor-blade cross-sectional area and rotor-channel area

Subscripts:

cr conditions corresponding to Mach number of 1

id ideal

m mean-radius value

u tangential component

x axial component

0,1,2,...,10 station nomenclature, fig. 1

Superscripts:

' absolute total state

* U.S. standard conditions

TURBINE DESIGN

As mentioned in the INTRODUCTION, this turbine was designed for requirements in the general area of small rocket-propellant pump drives. The following overall design values, which are corrected to U.S. standard sea-level conditions at the turbine inlet, were chosen:

Equivalent weight flow, $w\sqrt{\theta_{cr}}\ \epsilon/\delta$, lb/sec	0.03841
Equivalent blade velocity, $U_m/\sqrt{\theta_{cr}}$, ft/sec	444.7
Preliminary equivalent specific work output, $\Delta h/\theta_{cr}$, Btu/lb	47.58
Blade- to jet-speed ratio, ν	0.244
Stage speed-work parameter, λ	0.5

A preliminary design was made by using these values and assuming that all the weight flow passed through each stage; this design resulted in a turbine having three stages with a mean diameter of 4.54 inches. The stage temperature and pressure distributions through the turbine and the velocity diagrams were calculated.

Since leakage flow between stages, which consists of flow through the disk seals and annular flow that is pumped by the rotor, is known to occur, a simplified estimate of the flow through each stage was made. The amount of leakage flow was assumed to be equal to the total flow that could be passed circumferentially from one stage to another by using the static density of each stage, the mean rotor velocity, and the total cross-sectional area of the annulus. This resulted in a weight-flow variation through each stage. The stator area of each stage was adjusted to be compatible with the weight-flow variation, and no changes were made in the velocity diagrams. The change in stator areas, and, thus, in weight flow of each stage, resulted in a change in the overall specific work output of the turbine. As a result, the final overall design requirements of the turbine were as follows:

Equivalent weight flow, $w\sqrt{\theta_{cr}}\ \epsilon/\delta$, lb/sec	0.03841
Equivalent blade velocity, $U_m/\sqrt{\theta_{cr}}$, ft/sec	444.7
Equivalent rotative speed, $N\sqrt{\theta_{cr}}$, rpm	22,436
Equivalent specific work output, $\Delta h/\theta_{cr}$, Btu/lb	41.8
Overall total- to static-pressure ratio, P_1'/P_9	14.5
Blade- to jet-speed ratio, ν	0.244
Number of stages	3
Blade height, l, in.	0.265
Tip clearance, in.	0.007
Axial clearance between blade rows, in.	0.010
Overall turbine efficiency, η_s	0.63

The final stage design characteristics were as follows:

Design characteristic	Stage		
	First	Second	Third
Total to static efficiency	0.69	0.67	0.64
Total- to static-pressure ratio	2.04	2.37	3.00
Ratio of stage weight flow to turbine weight flow	1.0	0.74	0.90
Work output, percent of total	0.38	0.28	0.34

Partial admission losses that were not included in this study can be expected to reduce the stage efficiencies.

In the preliminary design, the work split among the three stages was assumed to be equal. It can be noted in the preceding table, however, that the final-design work split was unequal because of the weight-flow variation through the turbine.

In addition to the previously mentioned characteristics, the following assumptions and requirements were made:

(1) Velocity head at exit of each stage lost in diffusion

(2) Total-pressure loss for each stator of 4 percent

(3) Constant hub and tip radii through each blade row

(4) Constant blade angles for all stator blades

(5) Constant rotor-blade entrance and exit angles

The velocity diagrams for the turbine were constructed at the mean radius and appear in figure 1. This figure shows that the first-stage stator was designed to operate subsonic, but near choking ($V/V_{cr} = 0.918$), while the second- and third-stage stators were designed to choke.

Stator

The stator blades were designed to be similar to the first-stage stator blades of the turbine described in reference 5, which were designed to turn and accelerate the flow to near sonic velocity in a smooth coverging channel. The critical velocity ratios at the exit of each stator were 0.918, 0.988, and 1.082 for the first, second, and third stages, respectively.

The stator-blade profiles and solidities for all three stages were exactly the same; only the number of passages varied. The number of passages was 6, 10, and 22 for the first, second, and third stages, respectively. The percentage arc of admission was 11.7, 19.5, and 42.9 for the first, second, and third stages, respectively. The suction surface of the blade downstream of the throat was a straight line.

The resulting dimensions and profiles of the stator blades are presented in figure 2(a).

Rotor

The rotor-blade design presents a compromise between geometry, diffusion, and reaction. Since a reverse-flow turbine was being used, a primary consideration was that the geometry of the blade be symmetrical about a plane that passes

through the midchord of the blade parallel to the plane of rotation.

In order to obtain a low total diffusion, a high solidity of 2.63 was used. Also, by arbitrarily increasing the channel width to 0.053 inch at midchord from 0.049 inch at the leading edge (an increase of approximately 8 percent), it was assumed that some of the diffusion on the suction surface would be transferred to the pressure surface. For a rotor-blade chord of 0.25 inch, 150 rotor blades were required to give a solidity of 2.63. In figure 2(b) are shown the dimensions and profiles of the rotor blades.

The rotor blades were designed for constant relative velocity entering and leaving the blade. The values of relative critical velocity entering and leaving the first, second, and third stages are, $(W/W_{cr})_2 = (W/W_{cr})_3 = 0.538$, $(W/W_{cr})_5 = (W/W_{cr})_6 = 0.586$, and $(W/W_{cr})_8 = (W/W_{cr})_9 = 0.654$ (fig. 1).

Reentry Ducts

The reentry ducts were designed to reduce the flow velocity from the rotor to a low value before it is carried to the stator inlet of the next stage. A development drawing of the turbine at mean diameter showing the reentry ducts is presented in figure 3. The reduction in velocity was accomplished by a transition section that consisted of a 0.3-inch-long straight portion followed by an annular flare of 0.3-inch radius on the inner and outer walls. This design resulted in a flow path that increased in height from 0.265 inch at the rotor exit to 1.2 inches in the low-velocity portion of the duct, giving an area ratio of 4.5.

The reentry-duct inlet ends were placed arbitrarily (1) at the same circumferential position with respect to the trailing edge of a stator blade at one end of a stator row (position A, fig. 3) and (2) at the opposite end of the stator at a circumferential position corresponding to an extension of the straight portion of the stator-blade suction surface (position B, fig. 3). The two reentry-duct collectors and the exit collector were placed in the same manner.

Because of the reverse-flow design, the flow path to the subsequent stage was very short compared to the crossover-type reentry turbine in which the flow always enters the same side of the rotor. In the subject turbine, the airflow made only one turn of approximately 178° per stage, thus making the reentry ducts smaller than those of the crossover-type turbine. The exploded cutaway drawing of the 4.54-inch-mean-diameter three-stage reentry turbine in figure 4 shows the major components.

APPARATUS, INSTRUMENTATION, AND PROCEDURE

The apparatus used in the evaluation of the performance of this turbine consisted of an inlet and an exhaust systems, a speed-reducing gear box, and an eddy-current-type dynamomenter. Figure 5 shows the experimental turbine installation.

The arrangement of the apparatus is shown schematically in figure 6. High-pressure dry air was supplied from the laboratory air system. The air was heated by an electric heater so that the turbine-inlet temperature was 600° R and was filtered to remove dirt particles. After passing through the turbine, the air was exhausted into the laboratory low-pressure exhaust system. With a fixed inlet pressure, a remotely controlled valve in the low-pressure exhaust line was used to maintain the desired pressure ratio across the turbine. The airflow was measured by a calibrated flat-plate orifice located in the air-supply line.

The power output of the turbine was absorbed by an eddy-current-type dynamometer that was cradle mounted for torque measurements. The torque-force measurement was made with a calibrated commercial strain-gage load cell.

The rotational speed of the turbine was measured with an electronic counter in conjunction with a magnetic pickup and a shaft-mounted gear.

An inspection of the turbine made prior to testing showed that the turbine blading was not fabricated to the desired dimensions. All the stator flow areas and the rotor flow area were less than the design values. The area measurements of the first-stage stator were approximately 10 percent less than the design area. The second- and third-stage stator areas were approximately 7 and 3 percent less than the design values, respectively. The rotor flow area was also less than design, by approximately 12 percent. Although these area values are somewhat different from the design values, it was felt that these differences would not change the major results significantly.

Figure 3 shows the positions of the instrumentation. All pressures were measured with wall taps connected to electrical pressure transducers. Temperature probes were placed at the mean radius.

All data were recorded by an automatic digital potentiometer and were processed through an electronic digital computer. Experimental data were taken over a range of inlet total- to exit static-pressure ratio from approximately 7 to 32. At each pressure ratio, the turbine rotative speed was varied from 40 to 100 percent of the design equivalent speed in 10-percent increments of speed. Eighty-percent speed data were not taken, however, because of a severe vibration in the apparatus at this speed. The turbine-inlet temperature was approximately 600° R, and the inlet total pressure was approximately 125 pounds per square inch absolute. The friction torque of the bearings and seals was obtained by motoring the shaft and rotor (rotor in vacuum) over the range of speeds covered in this investigation.

The turbine was rated on the basis of static efficiency. The inlet total pressure was calculated from the weight flow, the inlet static pressure, and the inlet total temperature as follows:

$$P_1' = P_1 \left\{ \frac{1}{2} + \frac{1}{2} \left[1 + \frac{2(\gamma - 1)}{\gamma} \frac{R}{g} \left(\frac{w\sqrt{T_1'}}{P_1 A_1} \right)^2 \right]^{1/2} \right\}^{\frac{\gamma}{\gamma - 1}}$$

The single-stage turbine investigation was conducted similarly to that of the three-stage turbine. The exceptions were that (1) an airbrake absorption dynometer was used (described in ref. 6) and (2) only one pressure ratio across the turbine was used, this being near the pressure ratio across the first stage when the three-stage turbine was tested.

RESULTS AND DISCUSSION

The results of this investigation are presented in three sections. The first section, Overall Performance, presents the performance results for the complete turbine. The second section, First-Stage Performance, presents the results of testing just the first stage as well as a statement on the work split among the three stages. The third section, Weight-Flow Distribution, discusses the weight-flow distribution as a result of an analysis of the leakage flows.

Overall Performance

The overall performance of this turbine appears in figures 7 and 8. Figure 7 presents the variation of turbine specific work output $\Delta h/\theta_{cr}$ with total- to static-pressure ratio P_1'/P_9 for lines of constant blade speed. This figure indicates that, as the total- to static-pressure ratio was increased from 7, its lowest value, the specific turbine work output increased rapidly at first. With further increases in pressure ratio, the work output continued to increase, but not as rapidly; at the higher pressure ratios, the work output reached a limiting value for a particular speed. For design speed ($U_m/\sqrt{\theta_{cr}}$ = 444.7 ft/sec), the work output varied from 28.7 Btu per pound at a pressure ratio of 7 to a maximum of 41.3 Btu per pound at a pressure ratio of about 26. Work output remained constant at this maximum up to the maximum pressure ratio of 32. A specific work output of 38 Btu per pound was obtained at the design pressure ratio of 14.5, which was 9 percent less than the design specific work output of 41.8.

Figure 8 shows the variation of efficiency η_s with blade- to jet-speed ratio for lines of constant blade speed. This figure also shows a dashed curve drawn through the peak efficiency point of each speed line. This curve shows that, at the design blade- to jet-speed ratio of 0.244, the peak efficiency obtained was 0.57 as compared to the design value of 0.63. Figure 8 also shows that for each speed there was a large variation of efficiency with blade- to jet-speed ratio. The high pressure-ratio data are at the left portion of each curve in figure 8. As the pressure ratio was increased from the value where peak efficiency occurred, the curves broke away from the peak efficiency curve. This was caused by losses that occurred as the third stage approached limiting loading. As the pressure ratio was reduced from the value where peak efficiency occurred, the curves again broke away from the peak efficiency curve. This was caused by incidence losses that were becoming significant.

Figure 9 presents the variation of static pressure through the turbine at the different measuring stations (shown in fig. 3) for overall pressure ratios of approximately 7, 9, 15, and 32 at design speed. Also shown is the design pressure variation through the turbine. As shown in the figure, the measured

variation of pressure approximated the design variation of pressure. The first stage showed some overexpansion, which may have been caused by an area mismatch due to flow leakage losses from the first stage. The second-stage pressure variation was as designed. The third-stage variation showed underexpansion as a result of the fixed design overall pressure ratio and first-stage overexpansion.

The measured equivalent weight flow of this turbine was 0.03739 pound per second and was constant over the range of pressure ratios and speeds investigated, which indicates that the first-stage stator was choked. The first-stage stator flow coefficient was calculated to be 0.97. The measured weight flow was approximately 3 percent less than the design weight flow of 0.03841 pound per second for the first stage, which was designed to be near choking. As previously mentioned, the stator flow areas were less than the design values. Since the second- and third-stage stator areas were closer to design values than was the first-stage stator, choking of the first-stage stator resulted, although the second- and third-stage stators were designed for choking.

First-Stage Performance

To determine the percentage of the work being produced by the first stage, a test of the first stage alone was conducted. Figure 10 presents the performance results as a plot of static efficiency η_s against blade- to jet-speed ratio ν for a pressure ratio of 2.33. The maximum efficiency was 0.595, which is less than the design value of 0.69. As mentioned in the DESIGN SECTION, a portion of this efficiency loss was anticipated because partial-admission losses were not included in the design study. Additional efficiency losses may also have been due to the smaller than design flow areas that were mentioned in the section APPARATUS, INSTRUMENTATION, AND PROCEDURE. Data were taken at only one pressure ratio (2.33) - this being near 2.26, the pressure ratio across the first stage when the three-stage turbine was tested. With the assumption that the single-stage turbine efficiency was constant (0.595) for a small change in pressure ratio in the region where the curves of efficiency against blade- to jet-speed ratio are nearly flat, the specific work output of the first stage was computed to be 15.5 Btu per pound at the pressure ratio of 2.26. Although the work output is less than the design value, this stage produced 41 percent of the measured total turbine specific work output of 38.0 Btu per pound at design speed and pressure ratio. The obtained 41 percent of the measured total specific work corresponds to a design value of 38 percent.

The second and third stages were not tested as single-stage units because of the complexity of the inlet and outlet ducts of these stages. From temperature measurements taken during the complete-turbine tests, however, the indications were that the specific work output of the third stage was less than that of the second stage. No attempt was made to determine the actual work split.

Weight-Flow Distribution

A study was made to determine the weight-flow distribution through the turbine at design operating conditions. The choking weight flow through each stage

stator was determined experimentally to be 0.0374, 0.0290, and 0.0318 pound per second for the first, second, and third stages, respectively. These weight-flow values were corrected to the interstage pressures and temperatures that would exist if the complete turbine were operated at standard sea level inlet conditions. The second- and third-stage stators passed 77.5 and 84.9 percent, respectively, of the first-stage flow. As the flow passes through a stage, a portion of the flow is composed of leakage flow through the disk seals, leakage flow in the axial clearance spaces between the stators and rotor, and flow that is pumped to the next stage outlet. In order to compute these flows the following assumptions were made:

(1) For the total flow through both the upstream and the downstream disk seals, the stage outlet flow density was used.

(2) For the flow through the axial clearances and for the rotor pumping flow, the average density of a particular stage was used.

(3) The leakage flow in the axial clearance spaces between the first and third stages was assumed to be zero.

With these assumptions, an estimate of the leakage and pumping flows was made at the design operating point. The values of these leakage flows are given in table I as percent of turbine-inlet flow. The pumping flow for a particular stage was computed by the use of the equation

$$w = 12\rho_{av} l c U_m \Phi$$

Circumferential pressure gradients on the rotor, caused leakage flow from the first and second stages toward the center of the rotor through the disk seals. This flow leaked back into the third stage. This leakage flow (also the leakage flow in the axial clearance spaces) was computed by iterating with assumed values of flow coefficients until a balance of the weight-flow distribution through the turbine was obtained. This method resulted in a flow coefficient of 0.528 for the disk-seal flow. This appears to be a reasonable value, because the disk seal was a single sharp-edged restriction. The flow coefficient was assumed to be constant for the three stages.

When the annular flow in the axial clearance space was calculated, a flow coefficient of 1.265 was computed in the manner just described. The rotor, rotating in the same direction as the flow, caused the flow coefficient to be greater than 1. As mentioned previously, no flow was assumed to exist between the first and last stages.

Thus, it is seen that the leakage flows of this type of turbine play an important part in its performance, and they must be considered in the design. A simple estimate of the flows, like that made for this turbine design, appears to be a reasonable first estimate.

SUMMARY OF RESULTS

A cold-air experimental investigation of the 4.54-inch-mean-diameter three-stage reentry turbine yielded the following results:

1. An equivalent specific work output of 38 Btu per pound and a static efficiency of 0.57 were obtained at design speed and pressure ratio. The values corresponded to design values of 41.8 and 0.63, respectively. A maximum equivalent specific work output of 41.3 Btu per pound was obtained at and above a total- to static-pressure ratio of 26.

2. Experimental data from the first-stage tests indicate that the first stage produced 41 percent of the total turbine work output. Interstage temperature measurements made during the complete-turbine test indicated that the specific work of the second stage was greater than that of the third stage. The design work output of the first, second, and third stages, respectively, was 0.38, 0.28, and 0.34 of the total work output.

3. The measured pressure variation through the turbine approximated the design variation of pressure at the design operating conditions. The first stage showed some overexpansion and the third stage some underexpansion. The pressure ratio of the second stage was as designed.

4. The results of a weight-flow distribution study through the turbine at design operating conditions indicated that the second- and third-stage stators passed 77.5 and 84.9 percent, respectively, of the first-stage flow. The remaining flow was composed of internal flow leakage.

Lewis Research Center
National Aeronautics and Space Administration
Cleveland, Ohio, August 8, 1963

REFERENCES

1. Evans, David G., Guthrie, William D., and Wasserbauer, Charles A.: Design and Performance of a Six-Stage 8-Inch-Mean-Diameter Reentry Turbine. NASA MEMO X-487, 1962.

2. Wong, Robert Y., Darmstadt, David L., and Monroe, Daniel E.: Investigation of a 4.0-Inch-Mean-Diameter Four-Stage Reentry Turbine for Auxiliary Power Drives. NASA MEMO X-152, 1960.

3. Evans, David G.: Design and Cold-Air Evaluation of a Four-Stage 8-Inch-Mean-Diameter Reverse-Flow Reentry Turbine. NASA TM X-720, 1963.

4. Evans, David G.: Design and Experimental Investigation of a Three-Stage Multiple-Reentry Turbine. NASA MEMO 1-16-59E, 1959.

5. Rohlik, Harold E.: Investigation of Eight-Stage Bleed-Type Turbine for Hydrogen-Propelled Nuclear Rocket Applications. I - Design of Turbine and Experimental Performance of First Two Stages. NASA MEMO X-475, 1961.

6. Wong, Robert Y., and Nusbaum, William J.: Air-Performance Evaluation of a 4.0-Inch-Mean-Diameter Single-Stage Turbine at Various Inlet Pressures from 0.14 to 1.88 Atmospheres and Corresponding Reynolds Numbers from 2500 to 50,000. NASA TN D-1315, 1962.

TABLE I. - DISTRIBUTION OF LEAKAGE FLOW

[Percent of inlet flow.]

	Stage		
	First	Second	Third
Measured stator weight flow	100	77.5	84.9
Circumferential flow pumped by rotor:			
Out	13.2	6.5	2.6
In	2.6	13.2	6.5
Disk-seal flow:			
Out	8.0	1.4	0
In	0	0	9.4
Circumferential flow in axial clearance space:			
Out	3.9	1.8	0
In	0	3.9	1.8

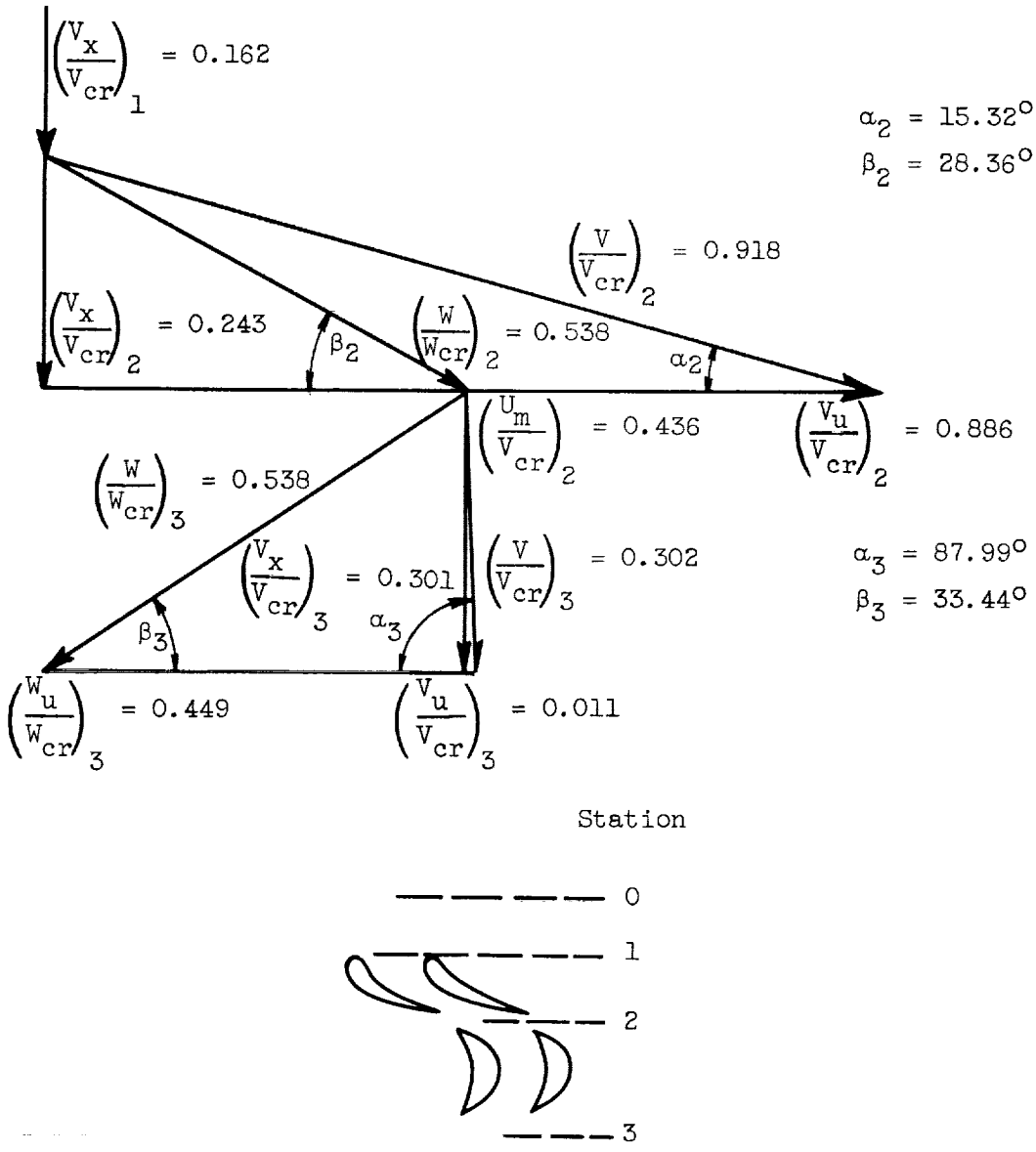

(a) First stage.

Figure 1. - Velocity diagrams for turbine at mean radius.

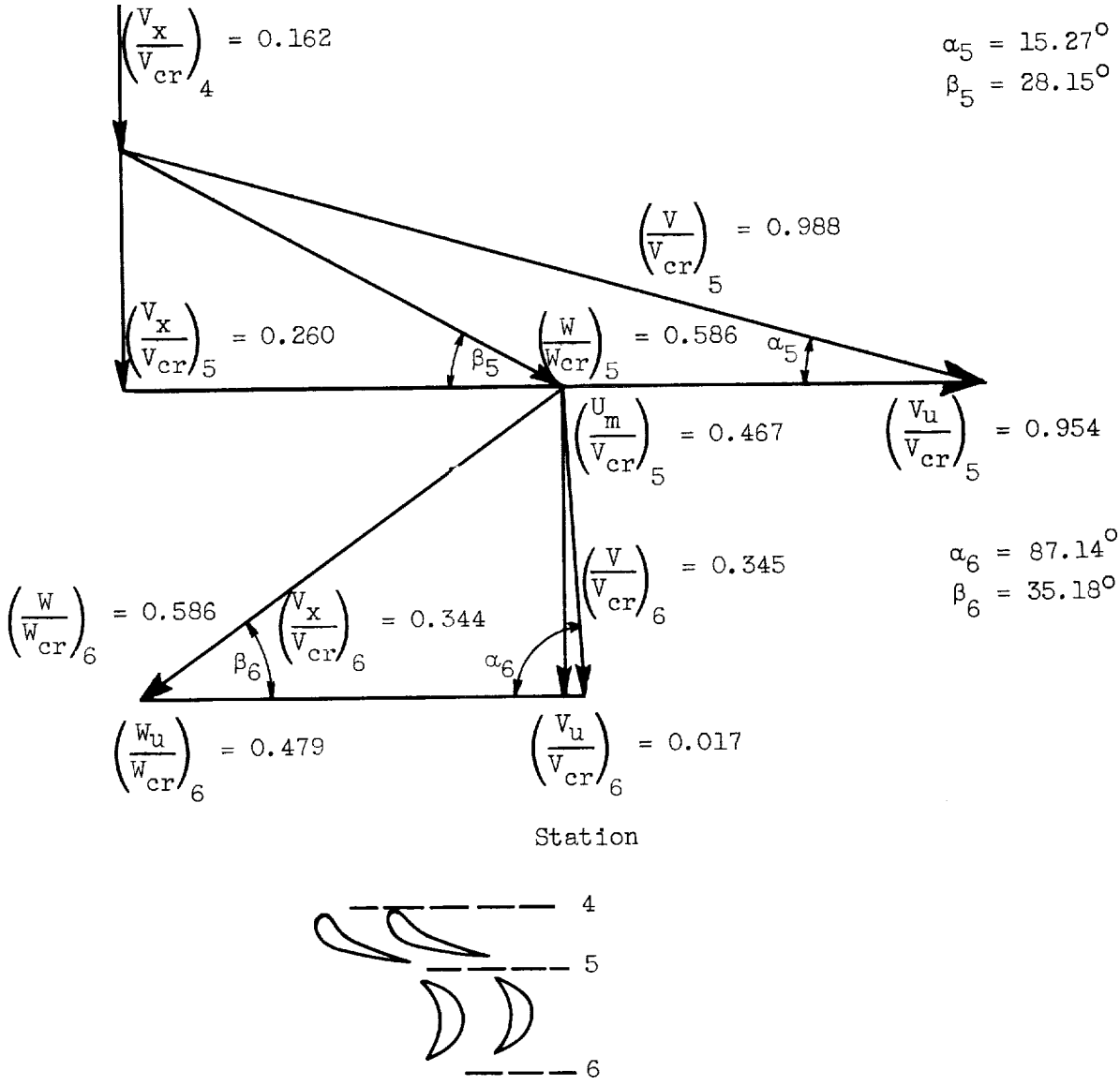

(b) Second stage.

Figure 1. - Continued. Velocity diagrams for turbine at mean radius.

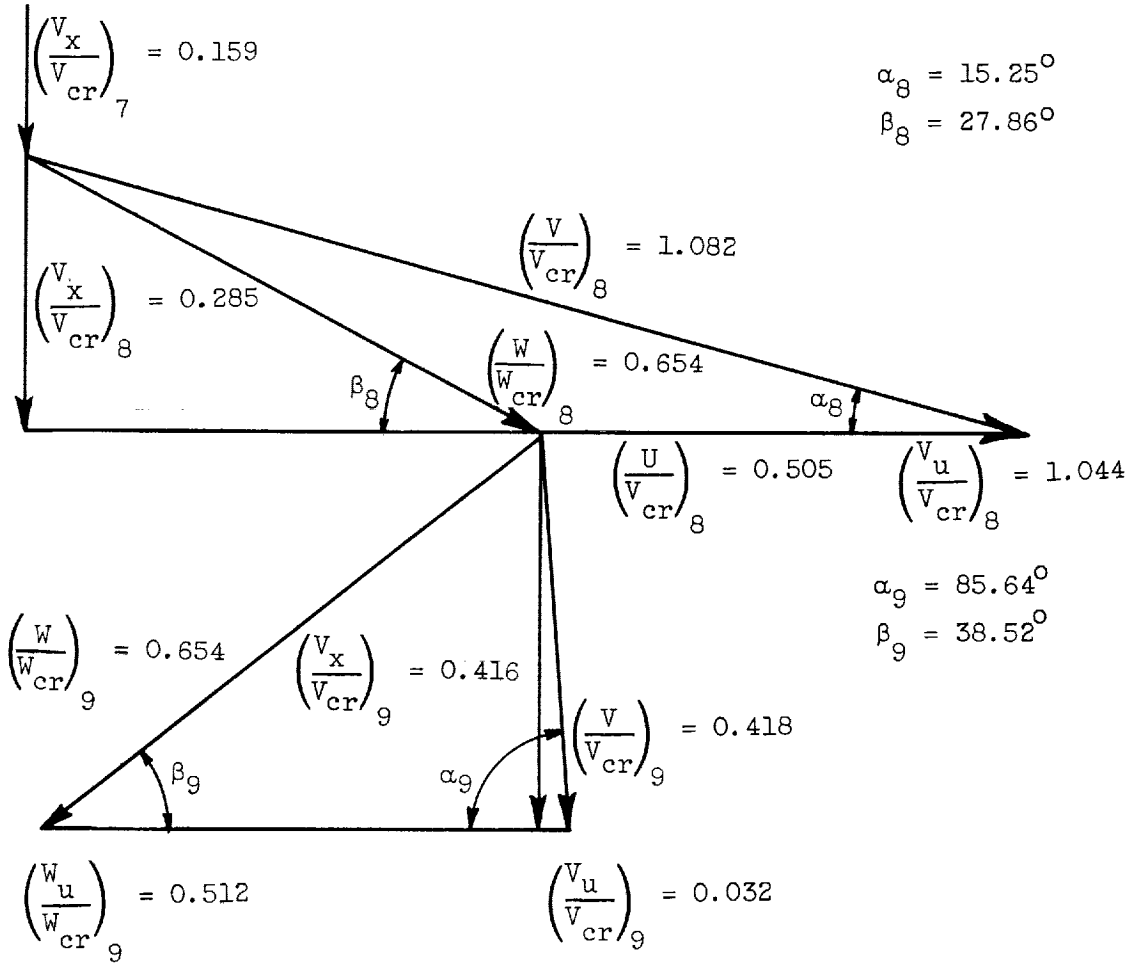

(c) Third stage.

Figure 1. - Concluded. Velocity diagrams for turbine at mean radius.

Stator-blade coordinates

X, in.	Y_L, in.	Y_U, in.
0	0.015	0.015
.040	.015	.075
.080	.034	.088
.120	.044	.088
.160	.048	.081
.185	.048	.076
.220	.045	
.260	.040	↑
.300	.033	Straight
.340	.026	line
.380	.018	↓
.420	.009	
.466	.006	.006

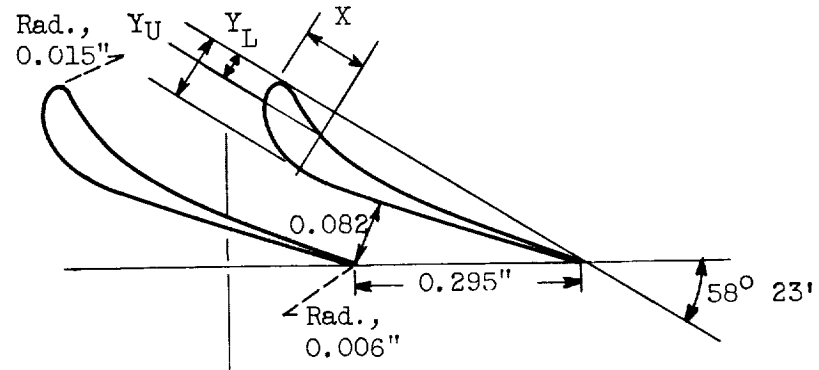

(a) Stator blade.

Rotor-blade coordinates

X, in.	Y_L, in.	Y_U, in.
0	0.0040	0.0040
.010	.0054	.0198
.040	.0402	.0634
.070	.0621	.1009
.100	.0738	.1199
.120	.0767	.1242
.130	.0767	.1242
.150	.0737	.1197
.170	.0667	.1087
.190	.0556	.0897
.210	.0395	.0623
.240	.0045	.0189
.2495	.0040	.0040

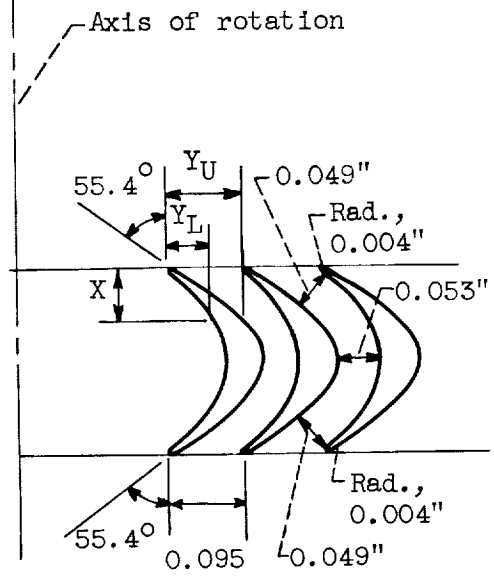

(b) Rotor blade.

Figure 2. - Stator- and rotor-blade geometry and coordinates at mean radius.

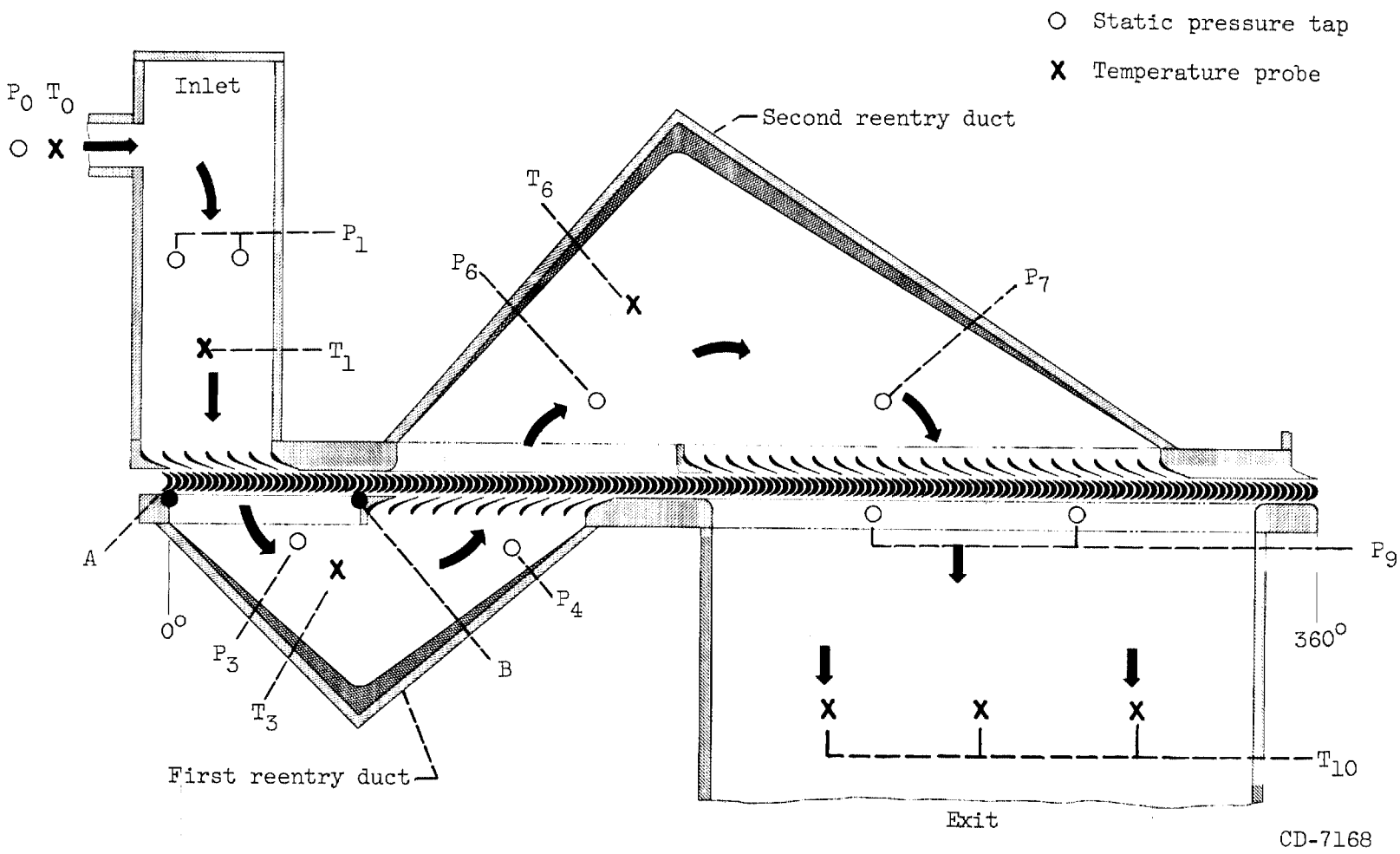

Figure 3. - Development drawing of turbine at mean diameter showing instrumentation.

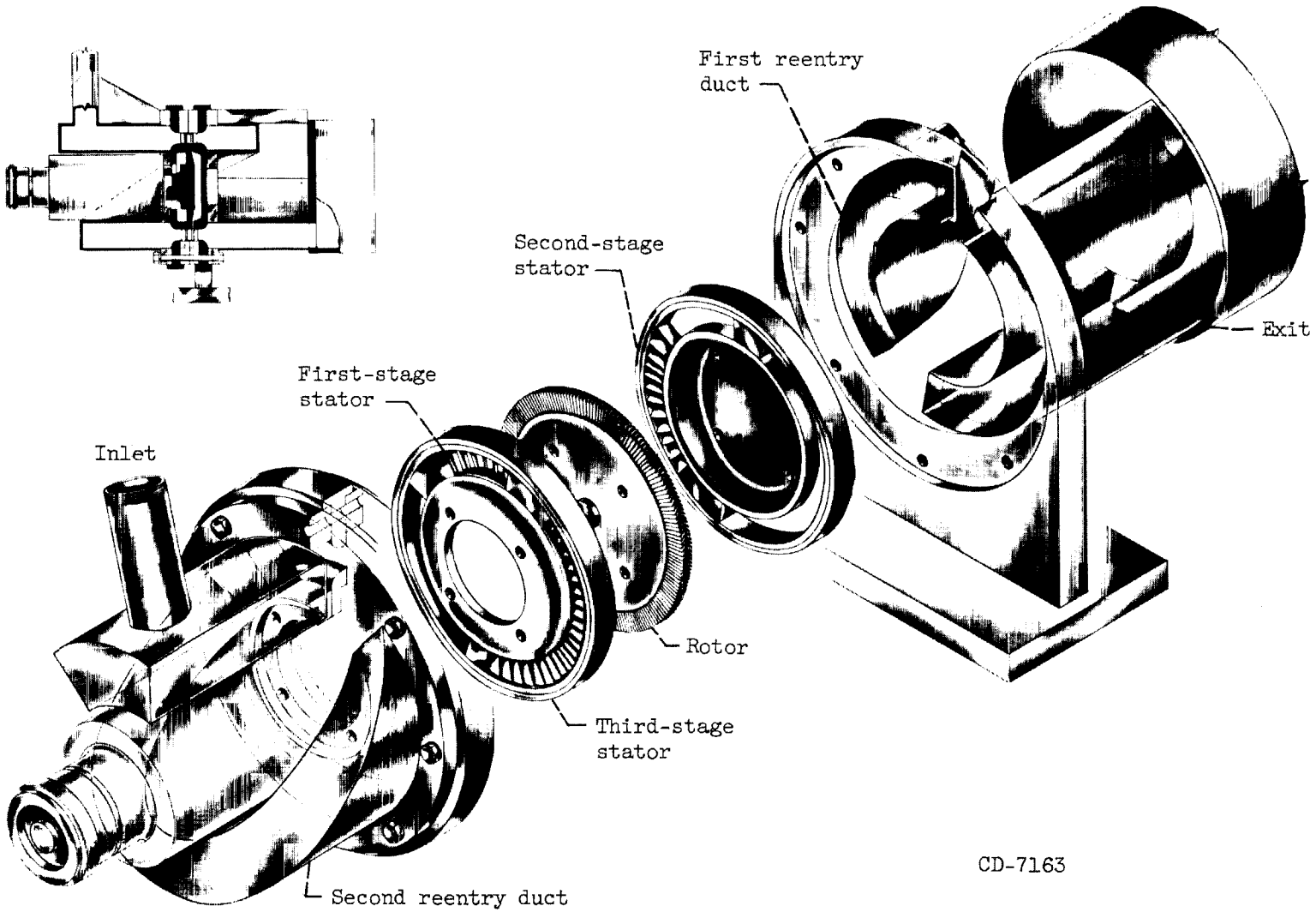

Figure 4. - Exploded cutaway view of turbine.

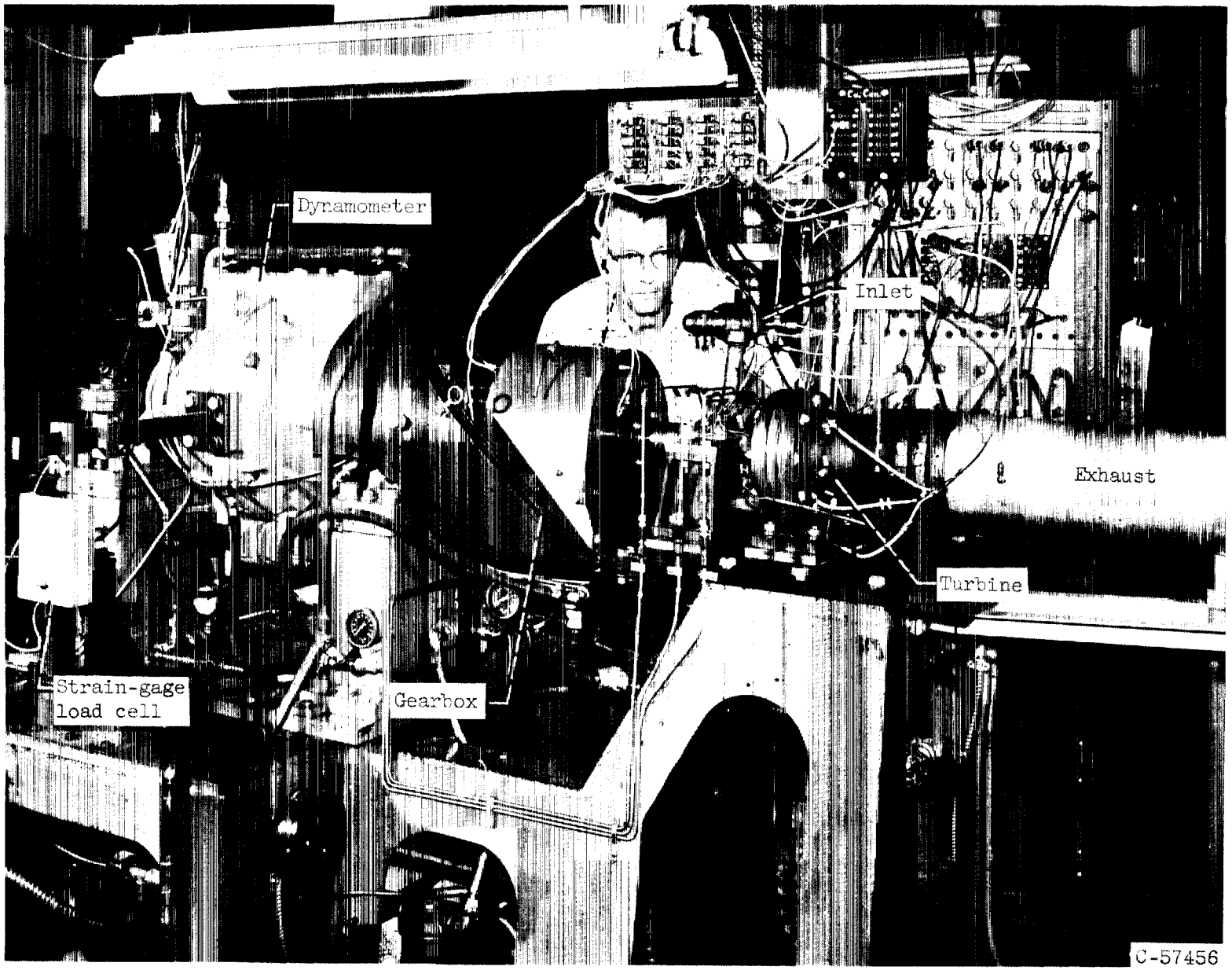

Figure 5. - Experimental turbine and apparatus.

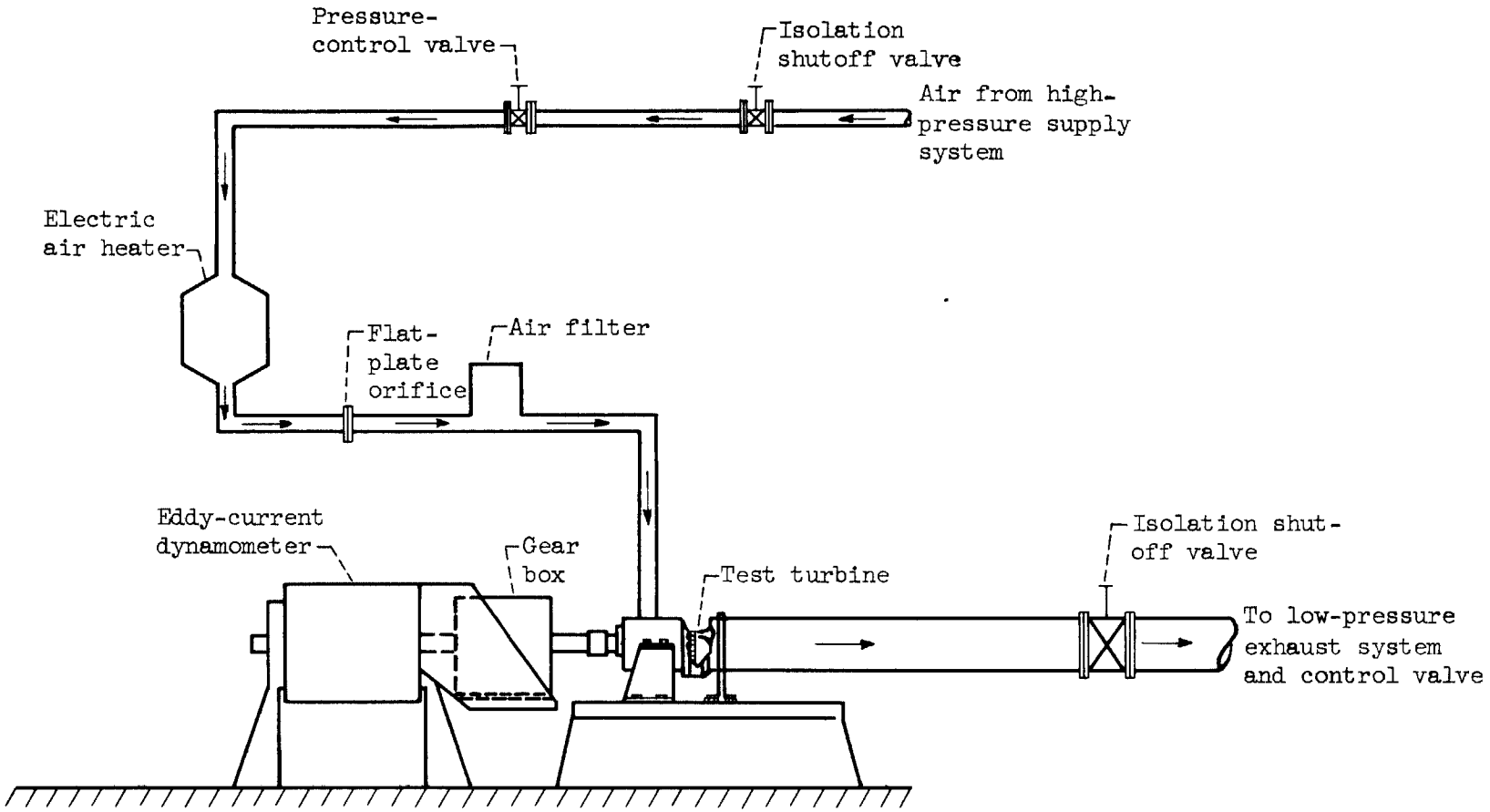

Figure 6. - Schematic sketch of experimental equipment showing airflow path.

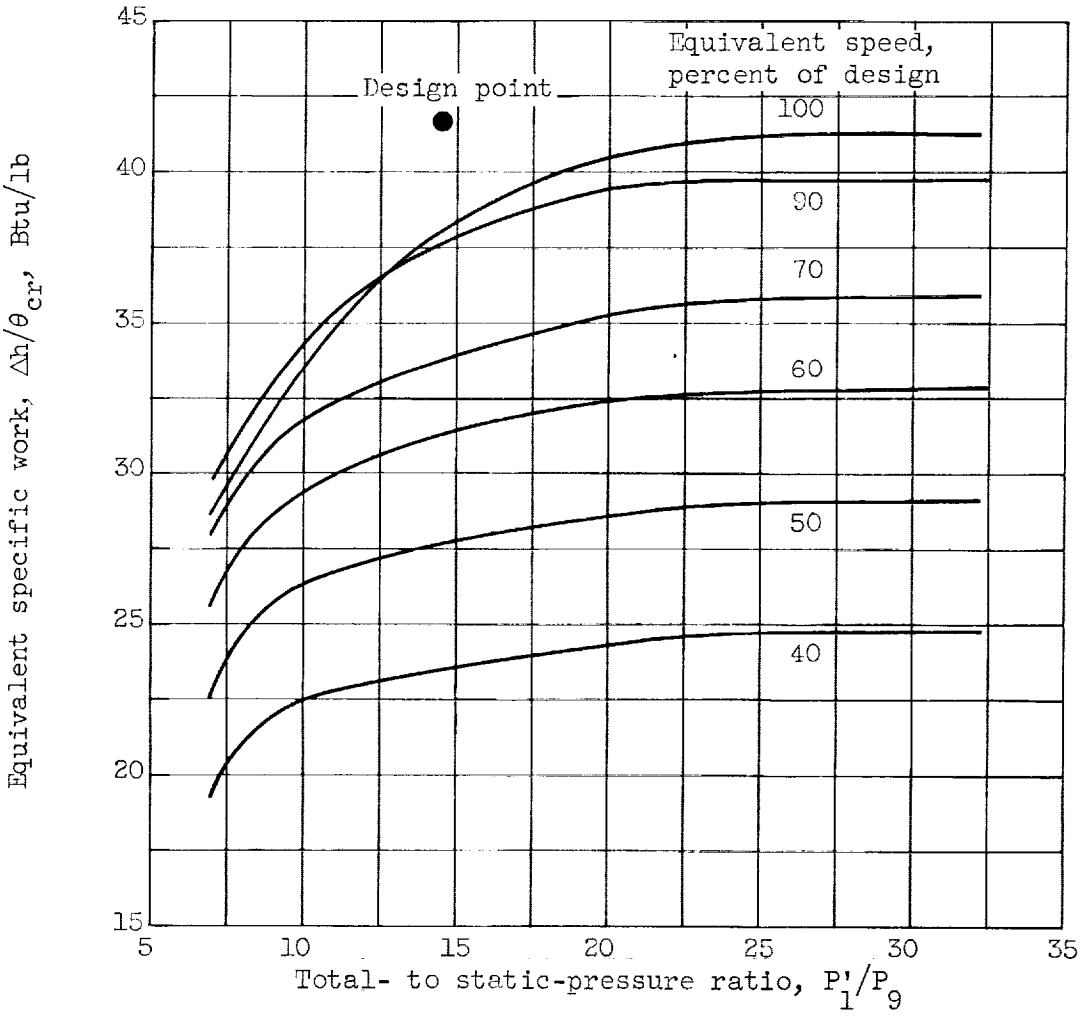

Figure 7. - Variation of corrected specific work with total- to static-pressure ratio.

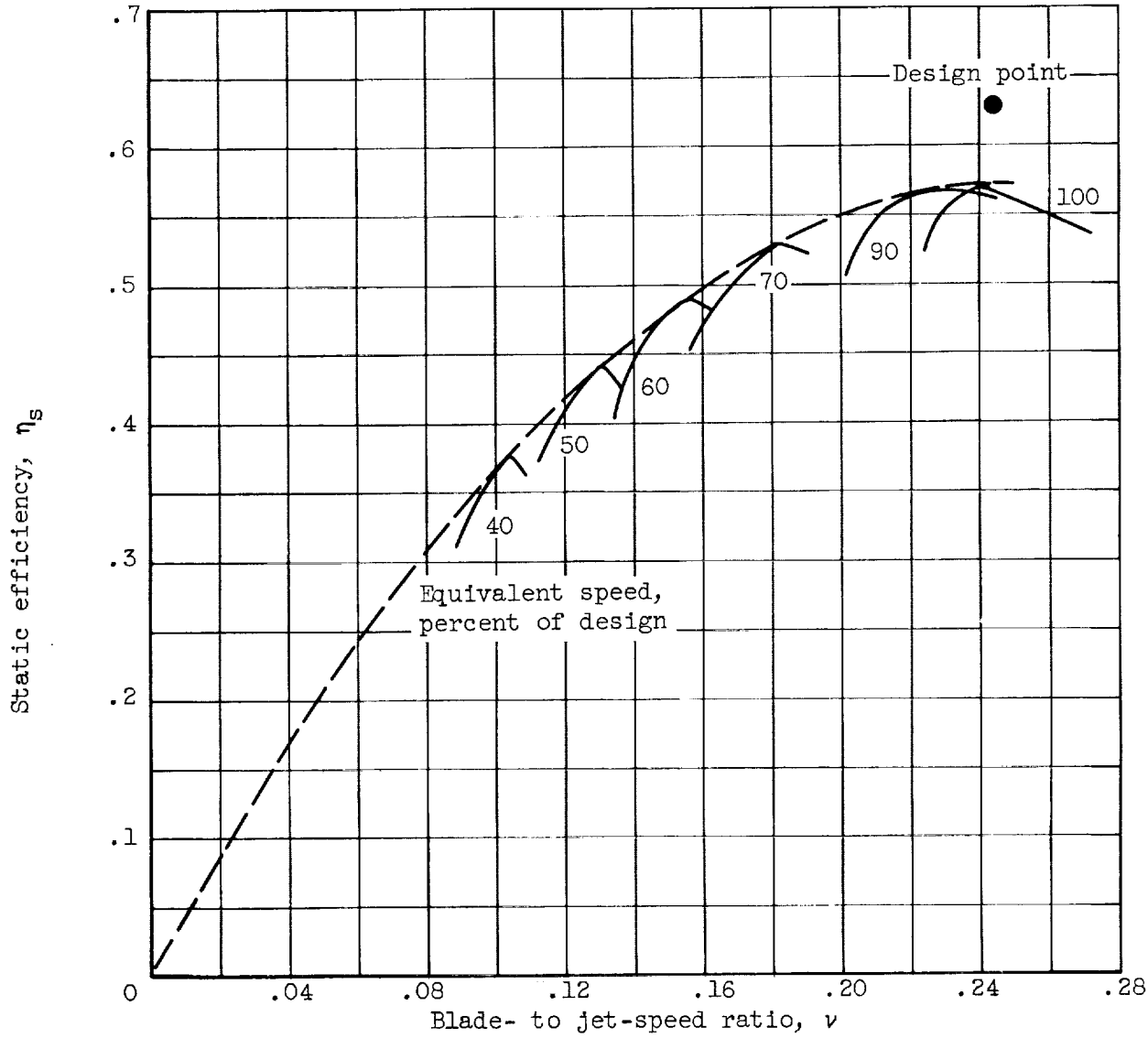

Figure 8. - Variation of static efficiency with blade- to jet-speed ratio for three-stage turbine over range of speeds.

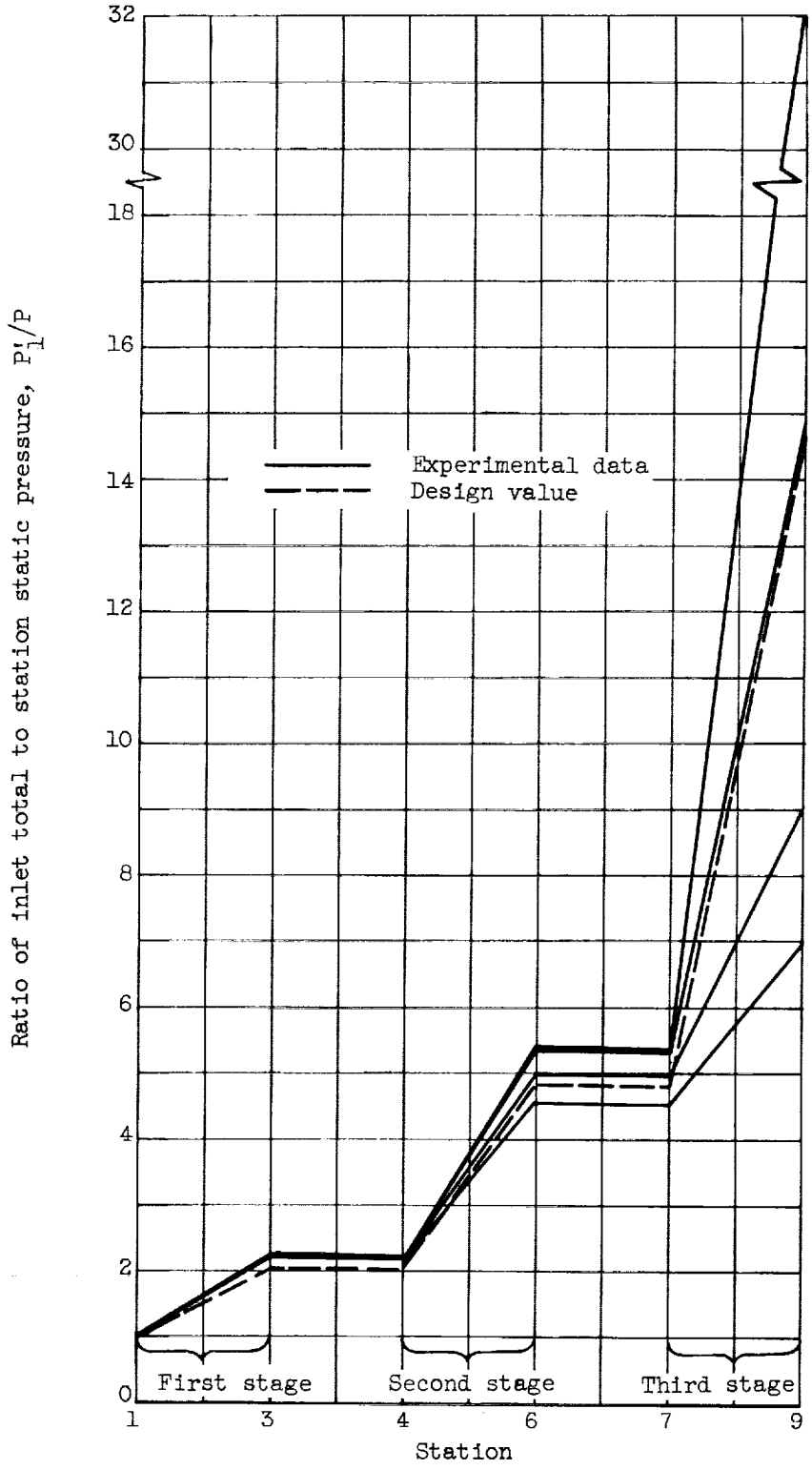

Figure 9. - Variation of static pressure through turbine. Design speed.

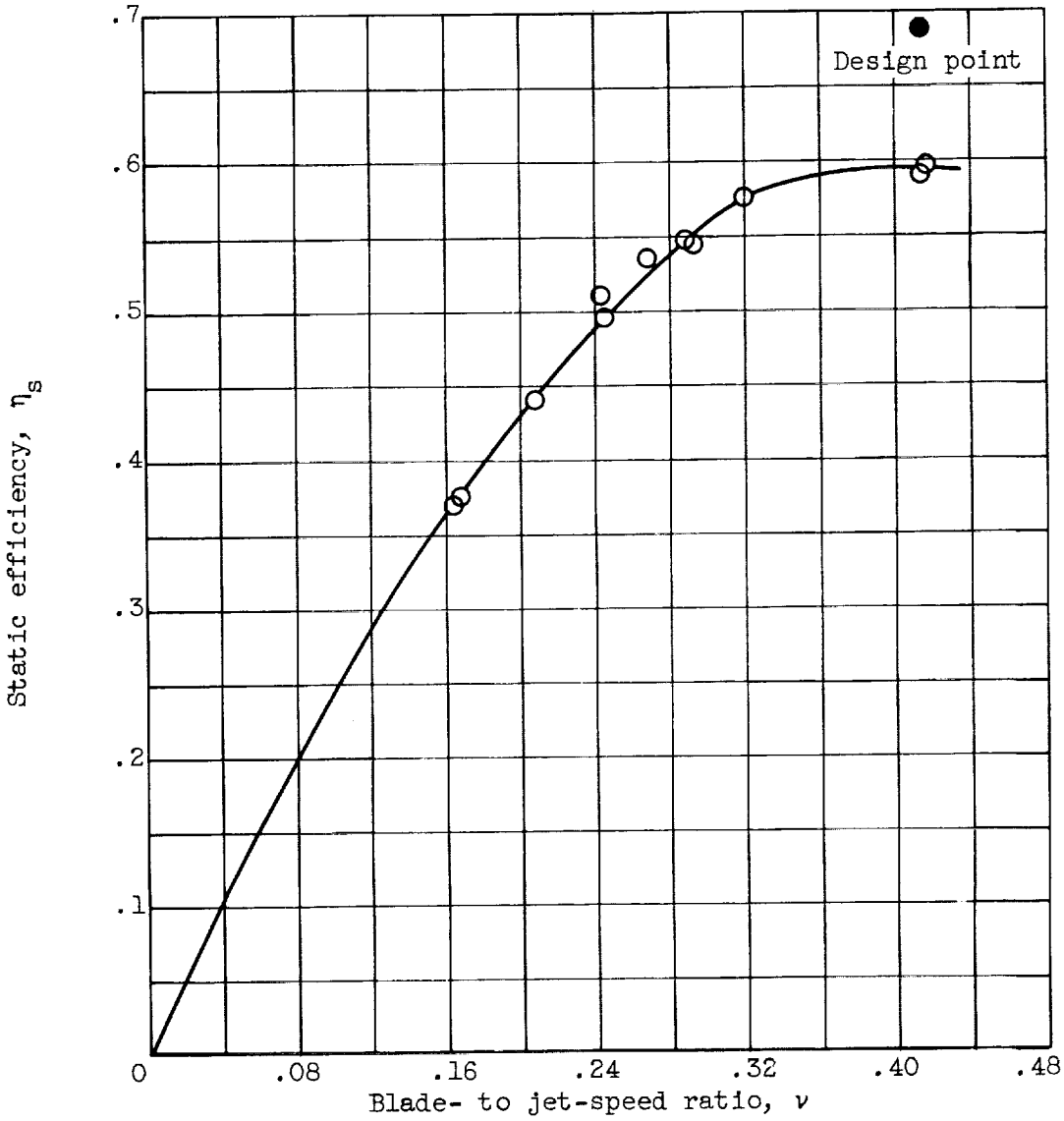

Figure 10. - Variation of static efficiency with blade- to jet-speed ratio for first stage at pressure ratio of 2.33.